Soil & Tillage Research 223 (2022) 105467

Contents lists available at ScienceDirect

Soil & Tillage Research

journal homepage: www.elsevier.com/locate/still

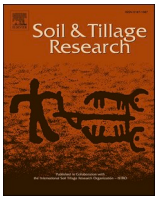

Dual-platform micromechanical characterization of soils: Oscillation shear rheometry and spherical indentation

Reza Hosseinpour-Ashenaabad [a,b,*], Thomas Keller [a,c], Mats Larsbo [a], Paul D. Hallett [d]

[a] Swedish University of Agricultural Sciences, Department of Soil & Environment, Box 7014, SE-75007 Uppsala, Sweden
[b] Ramboll, Geotechnical & Rock Engineering Department, Box 17009, SE-10462 Stockholm, Sweden
[c] Agroscope, Department of Agroecology & Environment, Reckenholzstrasse 191, CH-8046 Zürich, Switzerland
[d] University of Aberdeen, School of Biological Sciences, AB24 3UU Aberdeen, UK

ARTICLE INFO

Keywords:
Rheometry
Indentation
Micromechanics
Soil pastes
Viscoelasticity
Elastic modulus

ABSTRACT

The dynamics of soil structure is caused by biotic and abiotic processes, with the onset and magnitude of deformation controlled by soil rheological and mechanical properties. Quantification of such properties is challenging because soil behaviour changes with soil moisture, but common rheological tests are not applicable over all consistency ranges. Here, we combine oscillation shear rheometry with spherical indentation mechanical measurements of soil to obtain greater characterization over a broader range of water contents. The elastic modulus could be measured with either approach, with good agreement found for measured silt and clay textured remoulded agricultural soils. For shear rheometry, plastic viscosity, complex modulus and shear yield stress were also obtained. The spherical indentation provided measurements of hardness and yield stress. Although yield stress was correlated between approaches, the values were orders of magnitude greater for the indenter (0.54 ± 0.33 kPa vs. 34.4 ± 31.2 kPa), presumably because of different loading and failure conditions. At drier water contents, yield stress varied more between the two tests on the clay soil, which corresponded with brittle fracture creating artefacts in shear rheometry measurements. Spherical indentation has not been widely applied to the testing of soils, but the good agreement over a wide water content range between elastic modulus obtained from spherical indentation measurements (0.66 ± 0.27 MPa in wetter zone to 4.45 ± 2.53 MPa in drier zone) and shear rheometry (0.47 ± 0.11 MPa in wetter zone to 2.02 ± 0.98 MPa in drier zone) is promising. Moreover, spherical indentation can be applied to materials varying from brittle to viscous and allows testing on structurally intact soil aggregates. The geometry of a spherical indenter may more closely mimic contacting soil aggregates, so scope exists to extend the approach to explore the slumping of aggregated seedbeds produced by tillage.

1. Introduction

Soil tillage affects 12 million km^2 of the world's agricultural land with the aim to produce a mechanically loosened and ordered structure that improves crop productivity. However, the structure produced by tillage is short-lived, due to slumping and disaggregation over time, mainly caused by wetting and drying cycles (Bresson and Moran, 1995). These weathering processes break down soil fragments resulting in a smoother soil surface and fewer discrete soil fragments (Hallett et al., 1998; Carminati et al., 2007; Vogel et al., 2010). As soil aggregates coalesce and macropores shrink, significant changes in mechanical and hydraulic properties of soil occur (Bresson and Moran, 2004). These changes in soil structure can influence water infiltration, surface runoff, evaporation, and root growth with potentially large impacts on agricultural production and on the environment (Pires et al., 2008; Logsdon et al., 2013). Although soil structure of arable land is known to change drastically between tillage and harvest, the underlying processes that lead to these alterations are poorly quantified.

Nevertheless, there have been several attempts to incorporate soil structure changes over time in crop models (Roger-Estrade et al., 2009) and hydrological models (Chandrasekhar et al., 2018; Nimmo et al., 2021), including physically-based models of hydromechanical behaviour (Or et al., 2006). However, the complex array of weather and bio-geo-chemical processes in soil structure dynamics, coupled with

* Correspondence to: Department of Soil & Environment, Swedish University of Agricultural Sciences, Lennart Hjelms väg 9, Uppsala 75007, Sweden.
E-mail address: reza.hosseinpour@slu.se (R. Hosseinpour-Ashenaabad).

https://doi.org/10.1016/j.still.2022.105467

Available online 27 June 2022

mechanical behaviour that varies from viscous processes in wet soils (Ghezzehei and Or, 2001; Carminati et al., 2008) to brittle elastoplastic behaviour in dry soils (Hallett and Newson, 2005; Yoshida and Hallett, 2008) presents challenges. Consequently, most Earth system models generally assume soil structure to be static and the models are often parameterized with data collected at one time point (Fatichi et al., 2020).

Aggregate coalescence in wet soils is governed by viscoelastic processes that result from a combination of overburden pressure, gravity, and water potential gradients. Water intrusion, swelling, and shrinking can cause micro-cracking which facilitates further coalescence (Bresson and Moran, 1995; Ghezzehei and Or, 2000; Hallett and Newson, 2005). However, mechanical characterization of soil aggregate coalescence through viscous (Ghezzehei and Or, 2000) or elastoplastic (Yoshida and Hallett, 2008) processes typically relies on tests on remoulded soils where the inherent soil structure is lost. Remoulding of soil disrupts particle bonds, greatly reducing its mechanical stability compared to intact soil aggregates (Khaidapova et al., 2016). For wet soils, the samples are formed into pastes for rheological testing. Drier soils use samples formed into defined geometries with controlled crack sizes (Hallett and Newson, 2005).

At the wet end, rheological measurements with a shear rheometer acquires shear modulus, plastic viscosity, and shear yield stress (Ghezzehei and Or, 2000). Most of these studies have tested soil pastes, with an aim to explore properties that affect rheological behaviour such as organic matter (Stoppe and Horn, 2017), texture (Markgraf et al., 2006), clay mineralogy (Barré and Hallett, 2009) or biological exudates (Naveed et al., 2017). Tests with a parallel plate shear rheometer have been conducted on intact soils, sampled carefully from the field and trimmed to several millimetres thickness so that applied stresses were distributed through the sample (Pértile et al., 2018; Holthusen et al., 2019). Such a thin sample would be constraining if testing larger scale processes, such as interaggregate contact and deformation following tillage. Moreover, although shear rheometers have been used over a broad range of water contents, at the ductile to brittle transition, behaviour becomes erratic (Holthusen et al., 2017) and experimental error can increase due to poorer contact between the rheometer plates and the soil.

An alternative approach suitable to both the wet and dry end could be a spherical indenter, albeit with more limited material characterisation than a shear rheometer. A spherical indenter provides mechanical measurements of elastic modulus, hardness, and yield stress over a small contact area in repeated load-unload cycles akin to soil inter-aggregate contacts. Tests with a spherical indenter are commonly conducted on particle agglomerates like ceramics (Chen et al., 2016) and more recently on repacked soils (Naveed et al., 2018).

It is common to use more than one testing method to characterize the micromechanical behaviour of biomaterials (Canovic et al., 2016; Polio et al., 2018; Orbach et al., 2019; Lau et al., 2020), but these combined approaches have yet to be applied to characterise the micromechanical behaviour of soils. By deploying both shear rheometry and spherical indentation tests several micromechanical parameters can be obtained. Moreover, on both wet and dry soils, tests are needed that can accommodate intact specimens without complications from sample geometry, although surface roughness of aggregates at drier soil water contents will potentially affect the measurements. Indentation tests can be applied at the millimetre scale, which could enable measurements on intact soil aggregates. However, the indentation test on soils has not been evaluated against other measurement types of soil micromechanical behaviour, such as shear rheometry.

Common measurements of both shear rheometry and a spherical indenter are elasticity (often expressed as Young's modulus) and strength. But with a shear rheometer, greater characterisation of rheological behaviour, such as viscosity and the storage (elastic) and viscous (loss) modulus describes soil structure in greater depth. As described previously, the soil needs to be wet enough to flow for shear rheometry to be relevant, and remoulded samples are often tested. By combining shear rheometry with a spherical indenter, a "dual-platform" approach broadens the range of water contents that can be tested, with the spherical indenter allowing a comparison of shear rheometry to intact specimens and small-scale spatial measurements.

Here we evaluate this "dual-platform" characterization of mechanical properties. We apply oscillatory shear rheometry and spherical indentation measurements over a wide range of soil water contents, primarily putting emphasis on combining the testing methods for greater soil mechanical characterization. We hypothesize that Young's elastic moduli (E) obtained from shear rheometry and spherical indentation are similar, providing a pivotal parameter to link the testing platforms. In addition to greater mechanical characterisation from the "dual-platform" approach, another aim is to compare mechanical parameters that can be estimated by both methods (e.g., yield stresses) where there is overlap between approaches. Tests are limited to remoulded soil samples in this study to accommodate both oscillatory shear rheology and spherical indentation measurements. If both tests provide similar values for micromechanical parameters, there will be greater confidence to apply spherical indentation to intact soil fragments and soil aggregates at different scales where the mechanical soil structure index can be related to different soil structure types (Khaidapova and Pestonova, 2007). We use two soils with different texture and organic matter content over a range of water contents spanning viscous to elasto-plastic behaviour.

2. Materials and Methods

2.1. Soils

Spherical indentation and oscillation shear rheometry tests were conducted on soils sampled from two experimental arable fields near Uppsala, Sweden with different textures and organic matter contents (Table 1). The soils were sampled in April 2019 from the top 5 cm after seedbed preparation. After air drying at 40 °C, the soil was passed through a 1 mm sieve to minimise particle interlocking that may affect shear rheometry measured with parallel plates (Ghezzehei and Or, 2001). Sieved soil samples were then mixed with water to produce remoulded soils with gravimetric water contents (WC) within the range of 20–40 % (22, 24, 29, 32, 35, 37 %), which corresponds to a water potential range from − 200–0 hPa (Fig. S1). After thorough mixing to improve homogeneity, the soil samples were stored for 2–4 h in a fridge (4 °C) for equilibration to improve soil-water equilibrium (Likos and Lu, 2004; Matsushi and Matsukura, 2006; Salager et al., 2013).

Soils were tested as remoulded pastes of about 2.5 mm thickness, either smeared directly onto the lower platen of the rheometer or onto a petri dish for indentation tests. The paste was spread gently with a spatula and allowed to relax for 5 min before testing so that pore water would redistribute. The applied stress from the spatula was small enough to not cause water to drain from the soil matrix. No specific compaction was applied on samples before testing although inherent impacts from the testing setup such as axial force in the rheometer or indentation depth might affect the local bulk density. The data for bulk density are available for each sample (Table 2). During the tests, soil samples at different water contents were weighed immediately before and after the test, with the final water content verified by oven-drying for 24 hrs. The average soil water content reduction was limited to

Table 1
Clay, silt, sand, and organic matter composition for Krusenberg "clay" loam and Säby "silt" loam soils.

Soil Texture Class (Name)	*Clay (%)*	*Silt (%)*	*Sand (%)*	*Organic Matter (%)*
Clay Loam (Krusenberg)	36	38.85	25.16	2.37
Silt Loam (Säby)	26.76	54.5	18.8	3.66

Table 2
Dry bulk density of both soils are reported here for 6 tested water contents measured after each test.

Dry Bulk Density (g/cm3)	*Rheometer*		*Indentation*	
Water Content	*Silt Loam*	*Clay Loam*	*Silt Loam*	*Clay Loam*
22 %	1.3	1.23	1.11	1.17
24 %	1.72	1.58	1.63	1.73
29 %	1.55	1.57	1.76	1.48
32 %	1.46	1.54	1.46	1.4
35 %	1.54	1.41	1.53	1.52
37 %	1.49	1.24	1.43	1.36

0.3–1 % within the testing period.

2.2. Rheometry

Amplitude oscillation sweep tests under controlled shear strain were conducted on a HR-3 Discovery Hybrid Rheometer (TA Instruments, New Castle, DE, USA). The rheometer was fitted with 40 mm diameter hatched steel parallel platens to minimize slippage. Temperature was controlled at 20 °C by a Peltier module attached to the lower platen and by housing the rheometer in a controlled temperature room.

A layer of remoulded soil sample was placed on the lower platen and then the upper platen was lowered to a 2.5 mm gap distance. Any excess material was trimmed with a spatula. Tests were carried over the six soil water contents described in Section 2.1, enabling regression analysis. Axial stress was adjusted to + 0.7 N (~ +1 kPa) to produce initial confining conditions (Chen et al., 2010). During testing, the gap distance was maintained, and axial force was recorded. All tests were conducted under a constant angular frequency of 0.16 Hz based on ascending shear rate and total material deformation. Oscillation shear rate for strain-controlled measurements also varied from 0 to 1 (sec^{-1}) providing a suitable range of shear rates for Bingham model parameter calculations. There were 10 points recorded for axial stress and strain during the deformation strain ramp of 0.001 %– 120 % at a data sampling time of 3 s. These tests took approximately 20 min per sample. Drying from the small soil surface area at the edge of the platens was minimal and checked by measuring water content at the end of the test (Aguiar et al., 2018; Polio et al., 2018; Ettehadi et al., 2020; Holthusen et al., 2020). For our tests, shear storage modulus (elastic moduli) *G'*, shear loss modulus *G''* (viscous moduli), and complex shear modulus *G** were derived from the oscillation amplitude sweep.

2.3. Indentation testing

A spherical indenter with a 1.5 mm radius was fitted to a ZN5 test frame (Zwick Roell, Ulm, Germany). A 100 N load cell accurate to 0.1 % of applied load measured applied force, which was recorded with displacement on testXpert III software. Soil pastes approximately 2.5 mm thick were brought into close contact with the spherical indenter and then loaded at a constant displacement rate of 10 μm s^{-1}. To facilitate comparison of small strain elastic moduli between small-strain micro-indentation and shear rheology, we used a low indentation rate to provide quasi-static loading conditions during the experiments, as soil mechanical properties are typically strain rate-dependent (Stoppe and Horn, 2017; Holthusen et al., 2017; Polio et al., 2018; Naveed et al., 2018; Lau et al., 2020). There were 10 loading-unloading cycles in each test, with the indenter depth increasing by 0.1 mm at each cycle so that the final maximum depth was 1 mm. These tests took approximately 15 min. Drying was minimised by placing the sample beneath a petri dish lid that had a small hole cut in the middle for the indenter. Water contents were checked at the end of the test by oven drying. From the indenter measurements we derived hardness, unloading elastic modulus, and tensile yield stress.

2.4. Dual-platform mechanical characterization

The various mechanical properties of soil derived by shear rheometry and spherical indentation are illustrated in Fig. 1. Elastic modulus, *E*, is the parameter that was obtained from both testing methods and is therefore used here to provide a direct comparison between rheometry and indentation tests. A good correlation of *E* modulus between the two testing methods, when applied to remoulded soils, would provide confidence of the indentation test.

3. Determining soil micromechanical properties

3.1. Oscillation shear rheometry complex shear modulus $\mathbf{G}^*$ and the linear viscoelastic (LVE) range

The linear viscoelastic (LVE) range was determined from the *G'* curve, which is the most reliable modulus for the purpose as it is completely recoverable (elastic). Here we selected the tolerance range of deviation of *G'* from the value at low shear strain (initial plateau phase) with the TRIOS analysis software and the data table where we applied a ± 10 % strain deviation. From the end of the linearity limit of the LVE range, strain values corresponding to yield were extracted and the corresponding *G'*, *G''*, and *G** were then calculated. Due to a very close LVE range extent of *G'* and *G** modulus values, the LVE range of *G'* was used to calculate the averaged LVE *G** values (Aguiar et al., 2018; de Cagny et al., 2019; Holthusen et al., 2020).

3.2. Young's elastic modulus extracted from oscillation shear rheometry

Young's elastic modulus for the rheometer, E_{rheo} can be calculated indirectly from the LVE plateau's *G**(averaged over the LVE range) by:

$$E_{rheo}{}^{*} = 2G^{*}(1+\nu) \tag{1}$$

where ν is the Poisson ratio. We assumed that ν equals 0.33, as is commonly measured for loam soils. Values tend to be higher for clay soils (0.35–0.45) and smaller for silt and sandy soils (0.20–0.33) (Berli et al., 2006; Keller et al., 2016; Chen et al., 2018).

3.3. Plastic viscosity and rheometer yield stress calculation

Rheometer yield stress from shear rheometry was calculated using the Bingham viscoplastic model. Parameters of the Bingham model, namely plastic viscosity η_p and rheometer yield stress τ_y, were extracted from the quasi-plastic characteristic flow curves, where the intercept of the tangent at the inflection point of the shear stress curve provides τ_y, while the inverse of the slope of the tangent provides η_p. Eqs. 2 and 3 were used to calculate τ_y from shear stress τ and shear strain rate $\frac{d\gamma}{dt}$ curves. η_p was calculated from η^* instantaneous viscosity, which is equal to G^* (Eq. 4) times the angular frequency, ω (Ghezzehei and Or, 2001):

$$\frac{d\gamma}{dt} = \frac{\tau - \tau_y}{\eta_p} \tag{2}$$

$$\eta^{*} = \eta_p + \frac{\tau_y}{d\gamma/dt} \tag{3}$$

$$G^{*} = \omega\eta^{*} \tag{4}$$

3.4. Soil hardness and Young's elastic modulus derived from indentation

Soil hardness, *H* measures the resistance to plastic deformation and is given by the maximum force measured at the end of each loading cycle, F_{max} divided by the contact area of the indenter, A_c. It was obtained by first estimating the surface deformation depth h_s:

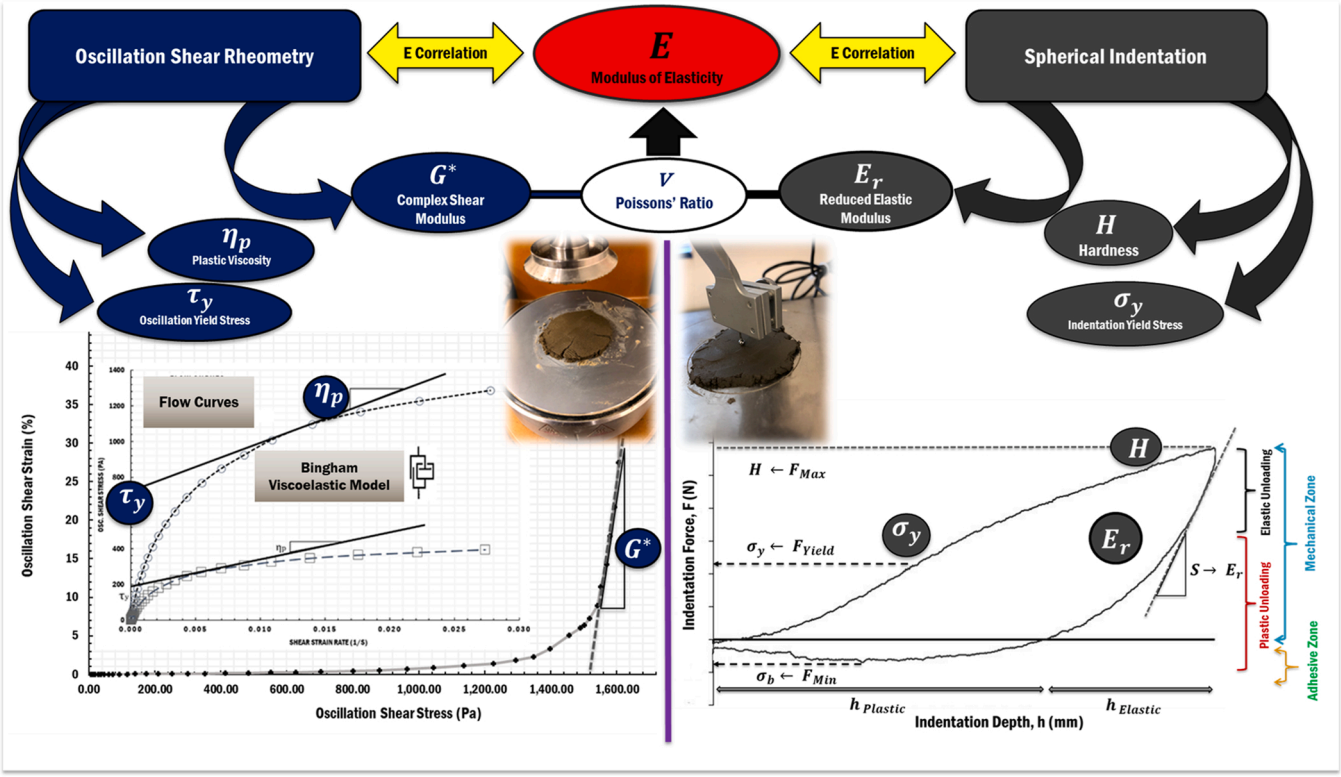

Fig. 1. Framework of a dual platform micromechanical characterization of soil with the pivotal parameter of elastic modulus as the link between the rheometer and the indentation test.

$$h_s = \varepsilon \frac{F_{max}}{S} \tag{5}$$

from F_{max}, the unloading stiffness (S) and a geometric constant ε that is equal to 0.75 for a spherical indenter. From this the contact depth (h_c) can be calculated by:

$$h_c = h_{max} - h_s \tag{5}$$

where h_{max} is the maximum measured deformation depth. Using h_c and the indenter tip radius R, A_c can be derived as:

$$A_c = \pi h_c(2R - h_c) \tag{7}$$

leading to the calculation of H:

$$H = \frac{F_{max}}{A_c} \tag{8}$$

Young's elastic modulus for the indenter E_{ind} was derived by first calculating the reduced elastic modulus, E_r:

$$E_r = \frac{S\sqrt{\pi}}{2\beta\sqrt{A_c}} \tag{9}$$

where β is the tip geometry correction factor of 1 for a spherical indenter, and then:

$$E_{ind} = E_r(1 - \nu^2) \tag{10}$$

where ν is assumed to be 0.33, as for the rheometer tests.

3.5. Indentation yield stress calculation

Yield stresses were extracted from the loading stress–strain curves at each loading cycle. The averaged axial yield stress over the first four indentation cycles provided the average indenter yield stress (σ_y) at each soil water content (Figs. 1 and 2). The method used here to extract the critical yield stresses is a combination of visual inspection and the method of 2nd derivative of the force – displacement curves within the viscoelastic region. Whereas τ_y and E_{rheo} derived from the rheometer are dominated mainly by oscillation shear deformation, σ_y and E_{ind} from the indenter can involve compressive, shear or tensile deformation depending on indenter depth and plasticity.

3.6. Data analysis

Regression analysis explored the relationship between mechanical properties and water content, fitting trends using 6 water contents and 1 replicate. Linear regression provided the best fit for most parameters, apart from yield stress, where there was a distinct exponential fit. In preliminary research on 3 replicates at a single water content, the coefficient of variation of mechanical properties was < 5 % for either soil, reflecting the sieved, homogenous samples that were used to test the approach. The relationship between mechanical properties obtained with shear rheometry and spherical indentation was also assessed by regression analysis. All data analyses were conducted with TRIOS software and Excel Microsoft.

4. Results

Fig. 2 provides an overview of the mechanical behaviour of the samples at different water contents for both oscillation shear rheology and spherical indentation. Each figure is plotted with strain on the X-axis, with the nonlinearity beyond a critical displacement evident for both tests. For oscillation shear rheology, the LVE range at low oscillation strain provides reliable measurements of G', G'' and G^*, with deviation from this plateau at greater strains providing yield stress and flow properties. In the indentation tests, shallower indentation cycles (<0.5 mm) produced similar H_{ul}, which we depict here as an LVE range as loading and unloading slopes remained constant. Consequently, we did not use the data from indentations > 0.5 mm.

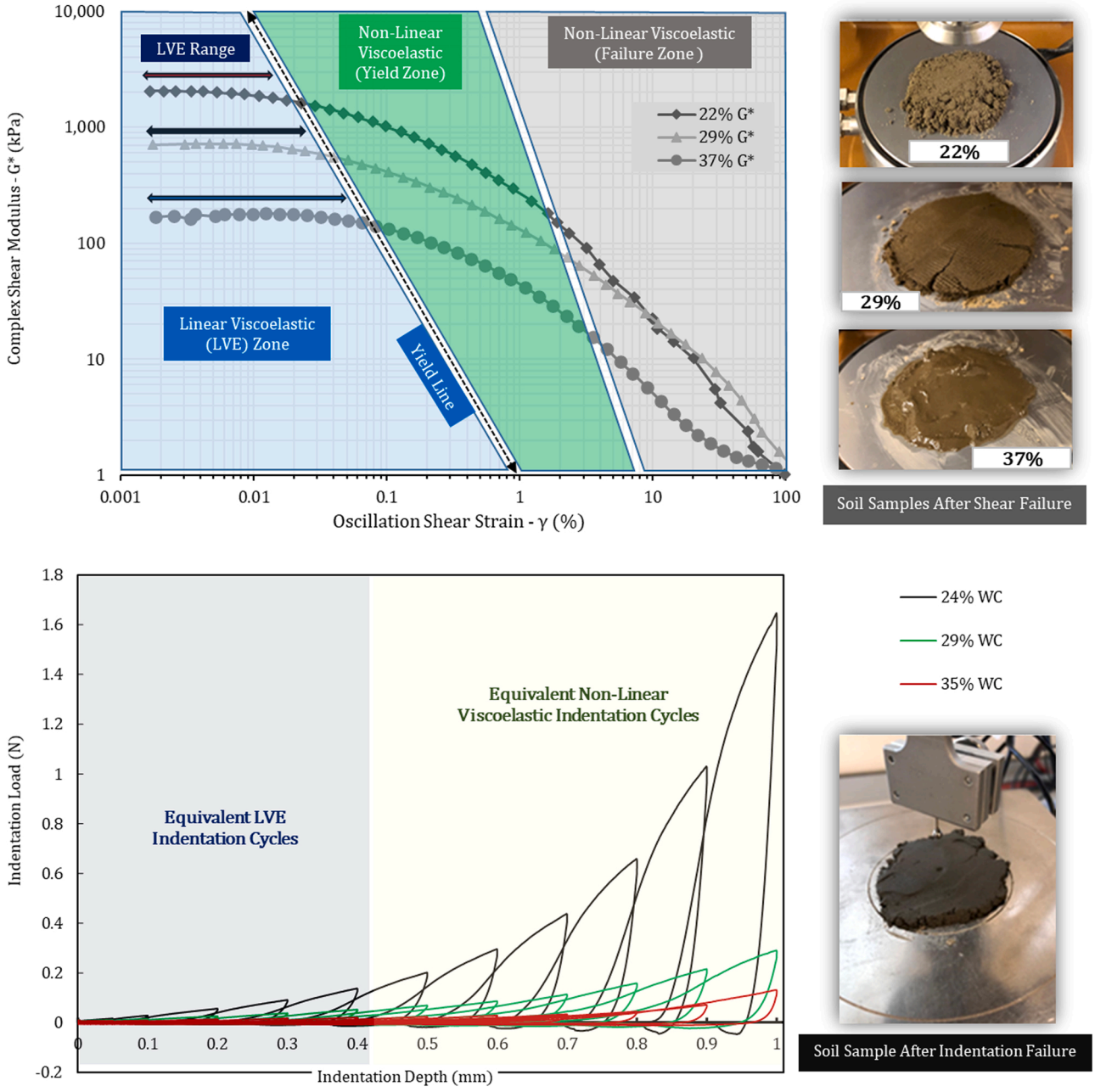

Fig. 2. Representative data from oscillation shear rheology (top) and spherical indentation tests (bottom) of Säby silt loam (silt soil) at a range of water contents. Three regions are defined for shear rheometry test outputs highlighting linear, nonlinear yield zone, and nonlinear failure zone, while two regions of equivalent linear viscoelastic and non-linear viscoelastic zones are defined for the indentation results. The photographs illustrate failure from brittle to viscous flow as water content increases in shear rheometry tests. The failure in indentation tests is very local.

4.1. Rheometry – plastic viscosity

η_p decreased with increasing soil water content for both soils (Fig. 3a). Generally, the correlations between plastic viscosity (η_p) and water content were strong, although the spread in the data for the clay soil was large at low water contents.

4.2. Yield stress values comparison between rheometer and indentation tests

Yield stresses derived from indenter and rheometer measurements are plotted together in Fig. 3b where for clay soil σ_y and $\boldsymbol{\tau_y}$ were ~ 0.8to1.2 kPa at soil water contents of 20–24 % with indentation yield stress larger in this drier water content range and then they dropped to ~ 0.2 kPa at high water contents of 32–40 % showing similar value ranges for both yield stress measurements. For both tests the correlation with water content was strong. For silt soil σ_y and $\boldsymbol{\tau_y}$ were significantly higher ~ 1.5–3 kPa at soil water contents of 20–24 % with rheometer yield stress $\boldsymbol{\tau_y}$ being larger in this drier water content range and then the values dropped to ~ 0.1–0.4 kPa range at high water contents of 32–40 % where again $\boldsymbol{\tau_y}$ value ranges were higher than indentation yield stresses σ_y by two folds. For both tests the correlation with water content was strong.

4.3. Indentation hardness

H as a function of water content is presented for both soils in Fig. 4. As with the other mechanical properties reported thus far, there is a

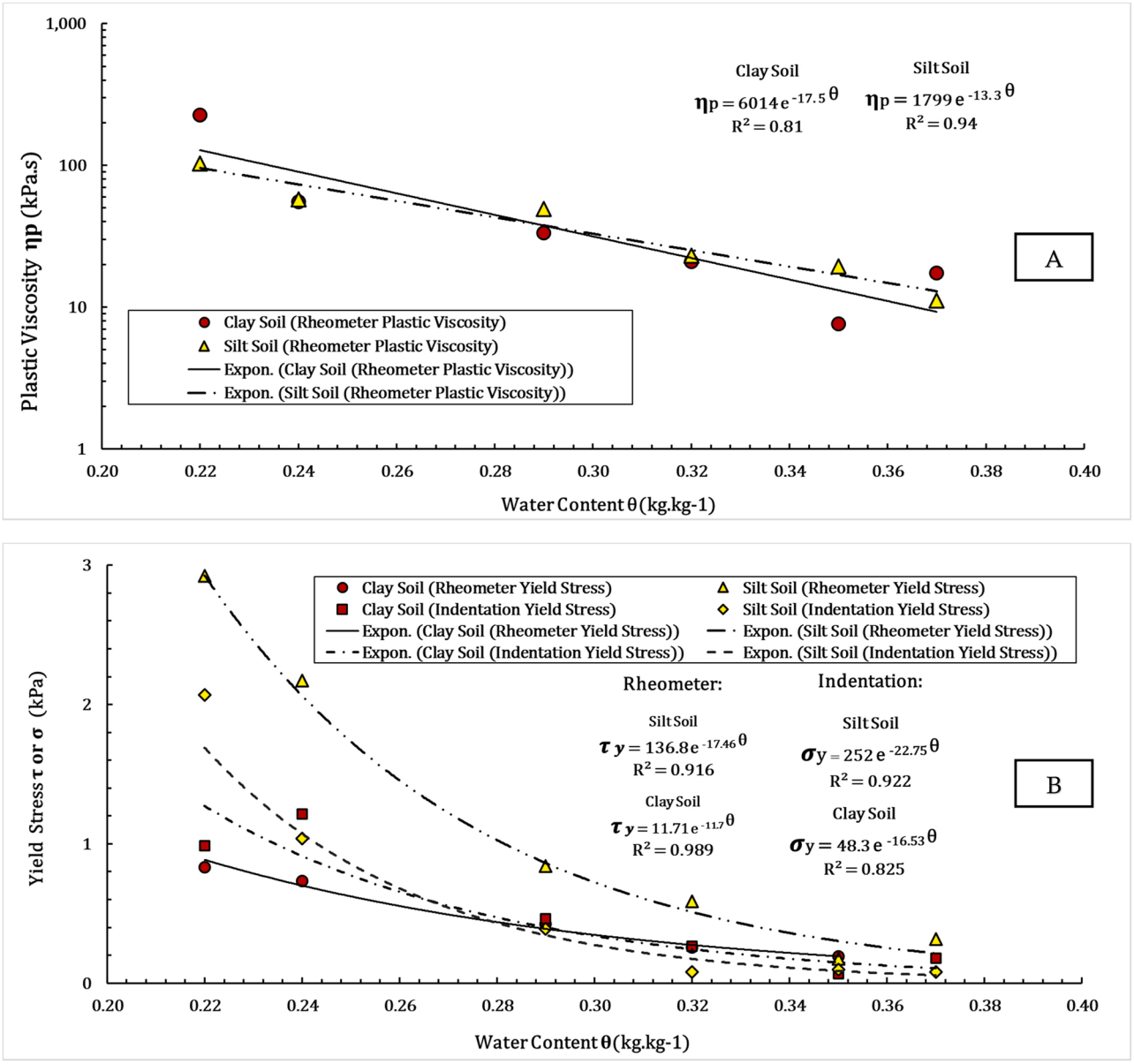

Fig. 3. Rheometer measurements of (A) Plastic viscosity and (B) yield stress as functions of water content for the two investigated soils. Yield stress trends for the indenter and rheometer are plotted to provide a comparison.

correlation between H and water content, with dry soils being about 10 times harder than wet soils and two soil types provide similar results.

A strong correlation between H and σ_y was found (Fig. 5), making it possible to have an initial estimate of σ_y from H instead of complex analysis from the force – displacement curves. The ratio of H/σ_y is along 2:1 ratio line for silt loam soil and along 3:1 ratio line for clay loam soil. Despite the strong trends that could be explored in between rheometer yield stress and soil hardness, hardness values were between 40 and 60 times larger than rheometer yield stress values. This was also depicted in Fig. 3b, where the yield stress values between indenter and rheometer are orders of magnitude different.

4.4. Relationship between indenter and rheometer measurements

Similar trends of elastic modulus versus soil water content were found for both methods (Fig. 6) resulting in a correlation between the two techniques that approached a 1:1 relationship (Fig. 7). At drier water contents this trend deviated, and clay soils consistently had greater E_{ind} than E_{rheo}.

σ_y and τ_y were also correlated (Fig. 3), albeit with different trends depending on the soil and substantially weaker stresses measured with the rheometer. Whereas the slope of σ_y and τ_y was almost parallel to the 1:1 relationship for clay soil, it deviated for silt soil.

5. Discussion

5.1. Young's elastic modulus – relationship between the rheometer and the indenter

Shear rheometer and indentation tests on soil pastes were comparable for common mechanical parameters, particularly Young's Elastic Modulus where the relationship was close to 1:1. For both tests these data were obtained at strains within the LVE range. The relationship between indenter and rheometer derived Young's Elastic Modulus was closer to 1 for wetter than drier soils, likely because shear deformation (e.g., shear bands and liquid flow) dominated (Chan and Lawn, 1988; Vaidyanathan et al., 2001). Tests on other materials (e.g., hydrogel polymers, lung tissues etc.) have also shown strong correlations between

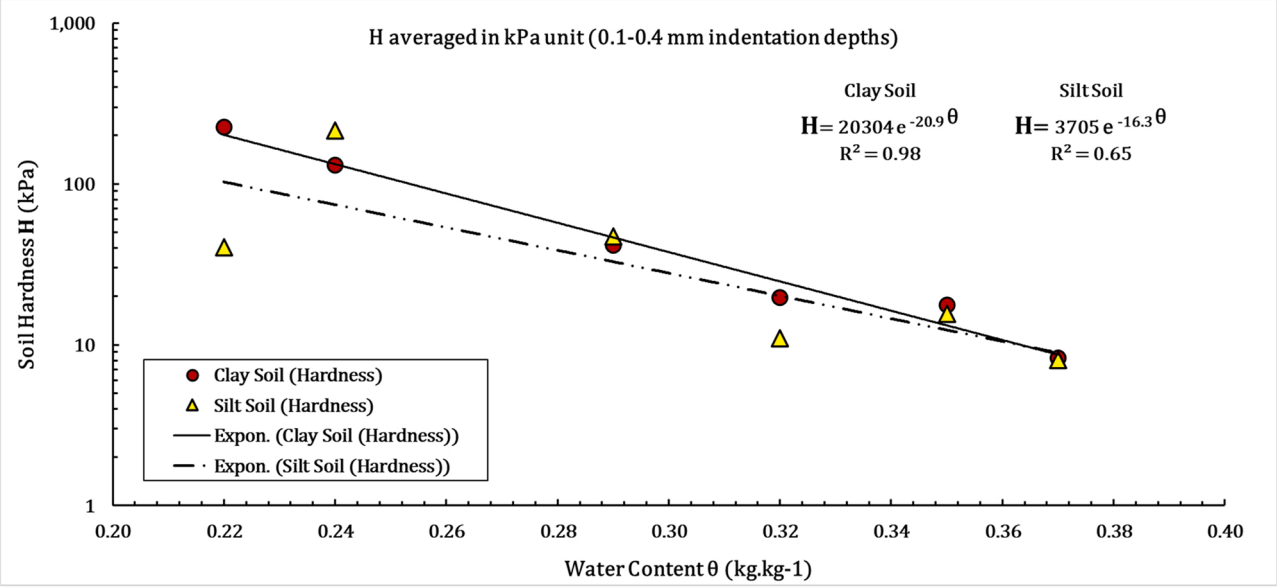

Fig. 4. Soil hardness measured with the indenter for Säby silt loam and Krusenberg clay loam at water contents ranging between 20 % and 40 %.

elastic modulus acquired from indentation and oscillation rheometer tests (Polio et al., 2018; Lau et al., 2020). The results suggest that indentation tests can provide reliable measurements of Young's Elastic Modulus at the small-scale.

The similarity of Young's Elastic Modulus between the rheometer and indenter tests is encouraging. Our data complements Naveed et al. (2018) by confirming that a spherical indenter provides accurate mechanical measurements that are comparable to larger scale tests within the LVE range. E_{rheo} was larger than E_{ind} for the clay loam soil, whereas the relationship was more scattered for the silt loam soil. The coarser particle size distribution of the silt loam soil likely increased particle interlocking that produces variability in micromechanical measurements obtained with a shear rheometer (Stoppe and Horn, 2017). As the soil dried, E measured with either testing approach also increased more for silt loam than clay loam soil (Fig. 6). This was likely driven by the combined effects of less lubrication by interlayer water and greater capillary stresses at a given water content for silt loam compared to clay loam soils (Fig. S1).

Given the geometry and small-scale of the spherical indenter versus the parallel plate rheometer, such a close similarity may be unexpected due to differences in deformation processes (Ghezzehei and Or, 2001; Naveed et al., 2018; Polio et al., 2018). E_{rheo} and E_{ind} have been found to be similar on other materials (e.g., hydrogels, lung tissue and brain tissue) where the elastic modulus measurements were closely related by 1–3x differences for lung and brain tissue measurements. These differences were attributed to microstructure differences and heterogeneity between tested samples, like here for soil. There are various sources of experiment error for both approaches. Particle interlocking has already been described, which would affect rheometer more than indenter measurements because of the confined testing conditions. For the indenter, the initial deformation has been found to be dominated by shear strains (e.g., shear bands) and affected by surface roughness and moisture in powders (Taylor et al., 2004; Stepniewska et al., 2020; Zafar et al., 2021). This was also evident in soil pastes tested at varying water contents where soil pastes behaviour varied from dry powder characteristics to fluid-like hydrogel characteristics. This shift from brittle to viscous behaviour of soil with water content makes it difficult to have a general multi-method characterization approach for soils. However, the promising initial results of Young's Elastic Modulus as compared between rheometry and indentation, for similar strain frequency and testing conditions, clears the path for exploring other micromechanical parameters between methods.

5.2. Yield stress relationship between the rheometry and indentation

Although, studies on other materials than soils (e.g., tissues, hydrogels, polymers) have found that elastic moduli are correlated between indenter and rheometer tests to a certain extent (Canovic et al., 2016; Polio et al., 2018; Orbach et al., 2019; Lau et al., 2020), there has been little focus on the correlation of yield stresses between these measurement methods. In this work, we can also compare yield stresses between rheometer and indentation tests of soils at a range of critical water contents. As yielding occurs outside of the LVE range, a one-to-one correlation would be unlikely as indentation results in a more complex deformation processes (involving both shear and compression) and tip friction (Lee and Radok, 1960; Vaidyanathan et al., 2001) likely contributed to the larger σ_y values compared to the rheometer τ_y values. Moreover, determination of σ_y from the 2nd derivative of the force – displacement curves within the viscoelastic region for the indenter may be less reliable than obtaining τ_y from G' in oscillating shear rheometry tests or from the Bingham viscoplastic model. The H/σ_y ratio between 1.7 and 2.5 for silt loam soil deviates from that predicted by the Tabor relation of 3, but H/σ_y of 2.4 and 3.2 for clay loam soil matches well (Koch and Seidler, 2009). The Tabor relation is mainly applicable to perfectly plastic materials. Therefore, the deviations from the ratio value of 3 might be associated with the contribution of elastic and viscoelastic soil deformations at higher water contents (Baltá-Calleja et al., 2004; Cheng et al., 2005; Fecarotti et al., 2012). The correlation between soil hardness and the indentation yield stress was strong and close to Tabor's relation of 3. Therefore, the discrepancy between rheometer yield stress τ_y and indenter yield stress σ_y likely arose from different boundary conditions, driven by compression and shear, between testing methods.

With the indenter, compressive/tensile yielding and shear yielding stress are combined as bulk yielding (Vachhani et al., 2013; Pathak and Kalidindi, 2015; Chang et al., 2018; Polio et al., 2018; Lau et al., 2020) whereas with the rheometer the controlled loading conditions impose mainly shear-based deformations (Ghezzehei and Or, 2001; Barré and Hallett, 2009; Sun et al., 2017). In conventional geotechnical tests on larger soil samples, the ratio of undrained shear strength to pre-compression stress varies from 0.2 to 0.3 for clay soils and 0.001–0.1 for sand-silt mixtures (Bro et al., 2013; Vardanega and Bolton, 2013; Persson, 2017). From the rheometer and indenter tests we found that this

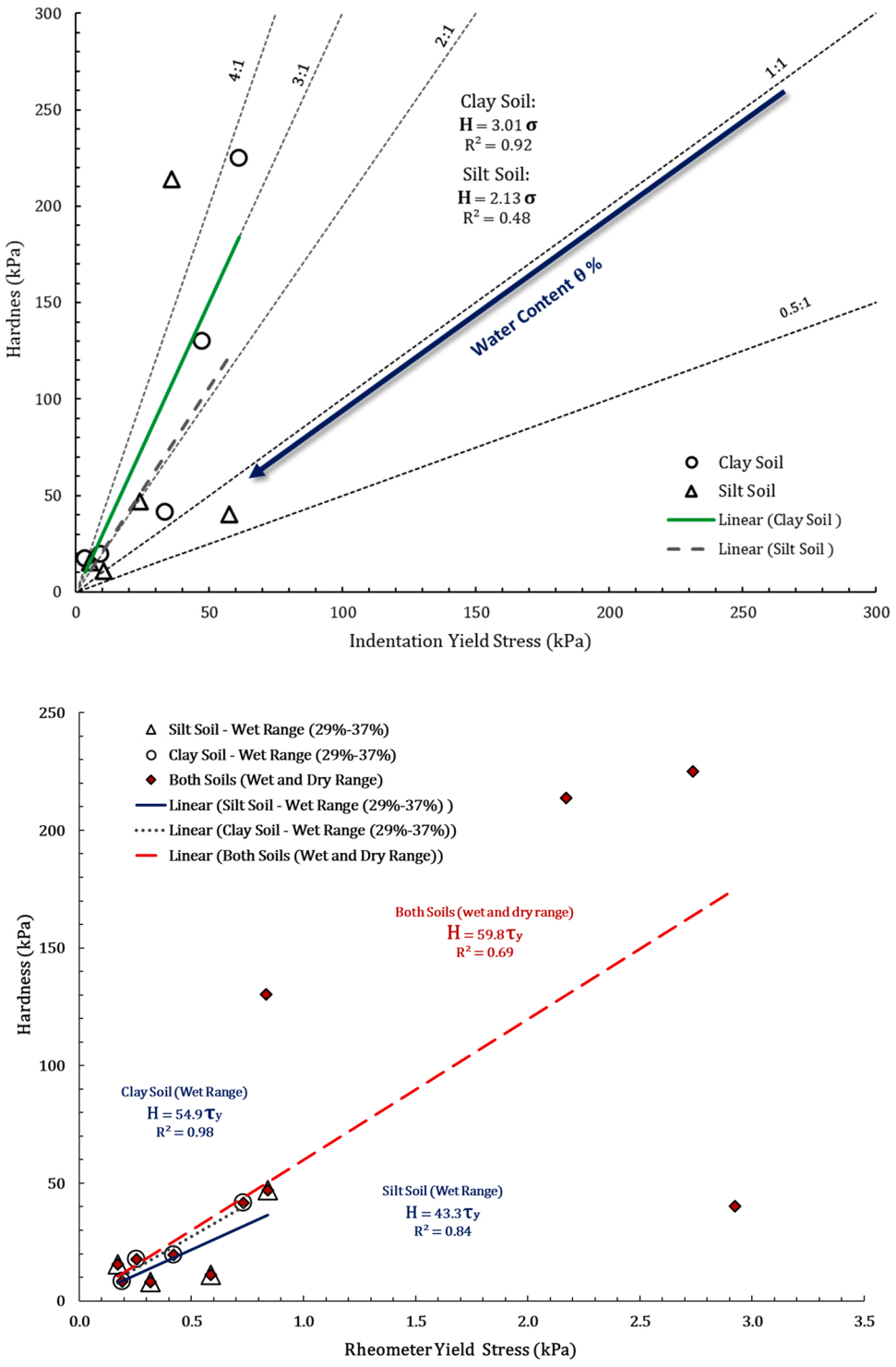

Fig. 5. The correlation between soil hardness and soil yield stress from indentation and rheometer tests for the range of soil water contents of the two tested soils. The dotted lines in the top figure show the 0.5, 1:1, 2:1 and 4:1 ratio between Soil Hardness and Yield Stress from the indentation tests.

ratio was between 0.1 and 0.2 for clay loam and 0.02–0.03 for silt loam soil (Fig. 3b). The difference due to soil texture was likely driven by the greater shear cohesion provided by clay versus silt and sand particles.

For both the rheometer and the indenter, yield stress increased with decreasing water content as many others have found for rheometer tests (Fig. 3b) (Ghezzehei and Or, 2001; Or and Ghezzehei, 2002; Yun et al., 2007; Transtrum and Qui, 2016; de Cagny et al., 2019). At the relatively large water contents tested, this would be partly driven by capillary cohesion by pore water pressure (Likos and Lu, 2004; Carminati et al., 2008). Based on pore water pressure alone, however, the yield stress of the clay soil (Fig. 3b) should increase more abruptly as the soil dries due to its water retention characteristics compared to the silt soil (Fig. S1). It is also evident that the indenter yield stress deviates more from the rheometer yield stress for silt rather than clay soil, suggesting further evidence that particle interlocking of the coarser silt soil could affect rheometer measurements.

In Fig. 3 it can be observed that τ_y followed a similar trajectory for clay loam and silt loam soil down to a water content of 0.26 kg kg^{-1}

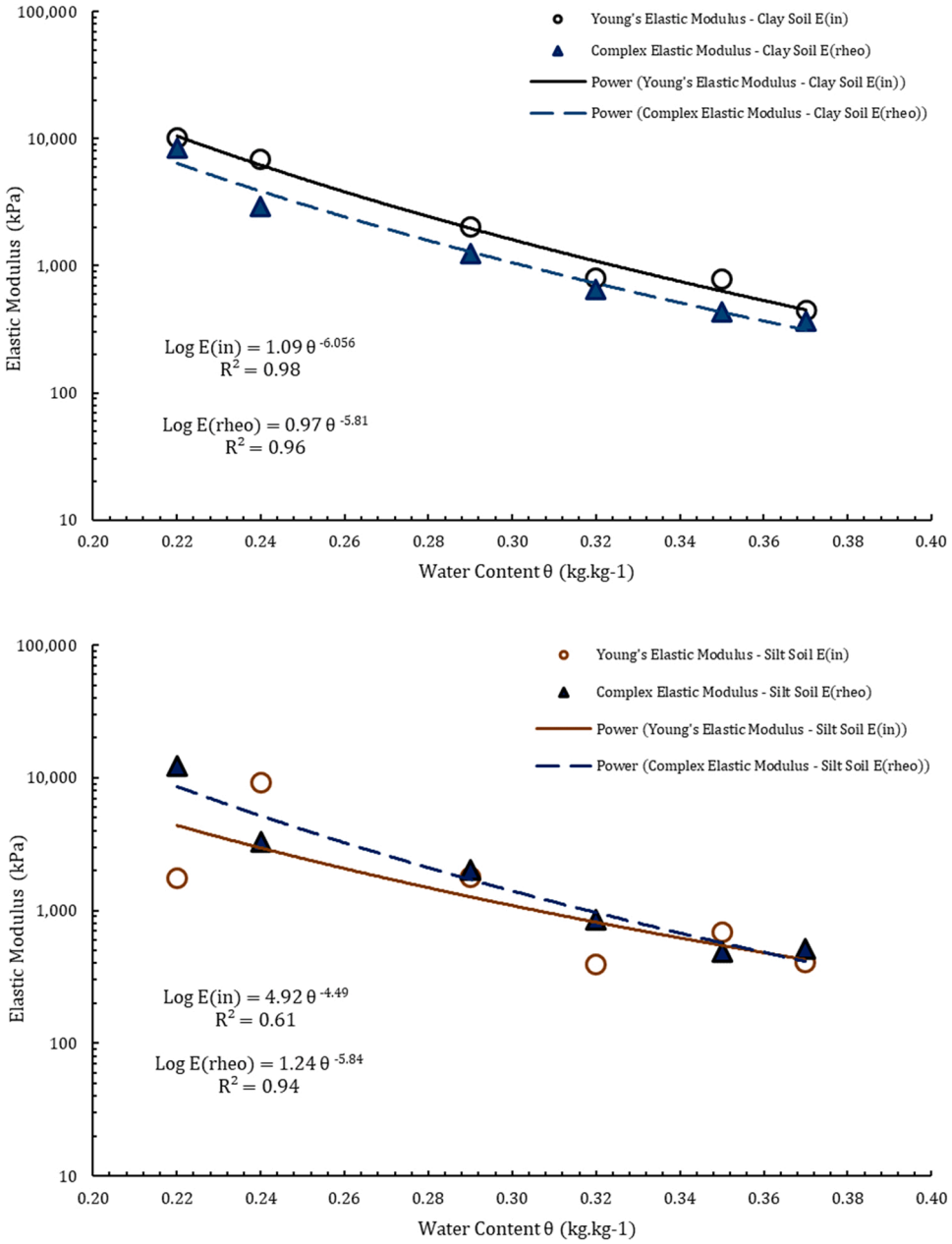

Fig. 6. Young's elastic modulus for the silt and clay soil acquired from amplitude sweep-oscillation shear rheology and steady-rate spherical mechanical indentation tests.

where the clay loam deviated. From oscillation shear ramp data (not shown), failure through brittle fracture occurred at these smaller water contents, so the soil no longer behaved as a visco-plastic paste that is a criterion for rheological measurements (Ghezzehei and Or, 2001). Indentation tests can be applied to viscous, plastic, and elastic materials (Chan and Lawn, 1988; Amidon and Houghton, 1995; Vaidyanathan et al., 2001; Taylor et al., 2004; Cheng et al., 2005) and a deviation in the trend of σ_y with water content was not observed in drier specimens.

5.3. Outlook

Therefore, combining both approaches has given confidence that the spherical indenter obtains realistic measurements, providing scope for its use on intact and dry specimens that cannot be tested with a shear rheometer. One potential application of spherical indentation is the testing of small-scale mechanical properties of soil aggregates or spatial measurements near the root-soil interface as suggested by Naveed et al. (2018). Although greater testing would be required to verify, the indenter has a geometry that likely reflects complex deformation between contacting soil aggregates better than oscillation shear tests with a rheometer. Where soil pastes are tested, the use of both a rheometer and an indenter, as a dual-platform characterization method, provides greater soil micromechanical characterization capability that will benefit the understanding and modelling of soil structure dynamics where shear, compressive and tensile components can be elaborated upon.

The rheometer provides many more mechanical properties derived from loading and unloading behaviour. Of particular use is η_p to characterise flow behaviour and model soil structure deformation over time. Our tests imposed cyclic loading and unloading cycles with the indenter, which should be explored further to derive rheological properties (Cseh et al., 1998). Although the rheometer can provide many more mechanical parameters related to elasticity, plasticity and viscosity, the reliability of these parameters needs greater scrutiny.

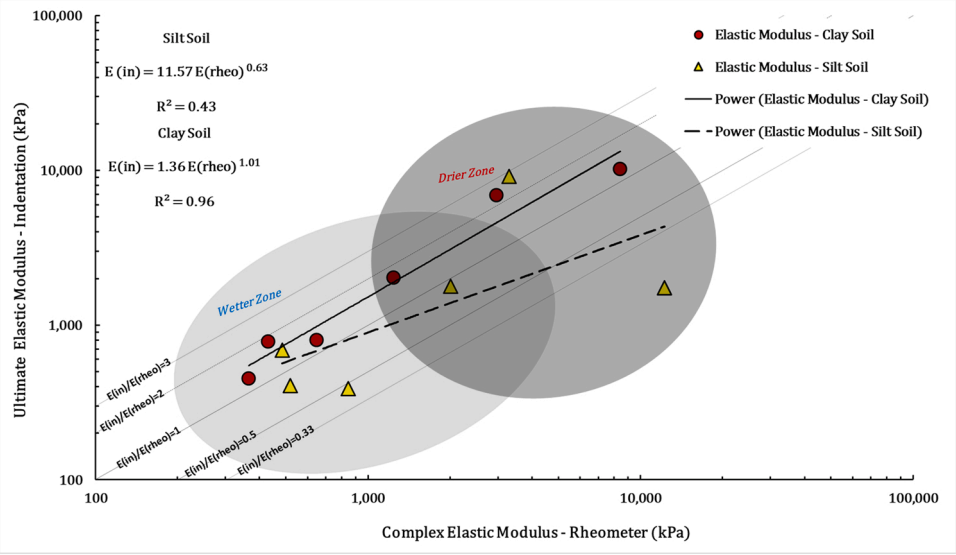

Fig. 7. Correlation between ng's elastic modulus for clay loam and silt loam soils acquired from amplitude sweep-oscillation shear rheology and steady-rate spherical mechanical indentation tests.

There are two potential limitations to the approach. Plate contact, particle locking in the thin specimen and a deviation from gel-like (flow) behaviour produces experimental errors (Ghezzehei and Or, 2001). Moreover, if pastes are tested, remoulding of soil disrupts the inherent structure of the soil, so the results may deviate considerably from undisturbed/structured soils. Holthusen et al. (2019) successfully used a parallel plate rheometer to test intact specimens. Future research could combine this approach with a spherical indenter that would be less constrained by sample geometry.

Certainly, the indenter has benefits in terms of testing small sample areas akin to inter-aggregate contact points. A weakness of the indenter method is the impact of rough soil surfaces affecting contact of the spherical indenter. At wet water contents this may be less of a problem due to initial plastic deformation, but below 24 % water content our tested aggregates had brittle fracture mechanical failure patterns. Surface roughness impacts on stress concentration requires further investigation, but similar impacts may occur in the field between contacting aggregates under stress from machinery or overburden. Other processes to explore include strain hardening under repetitive loading and weakening of soil under rapid wetting.

6. Conclusion

A very good correlation was found between shear rheometer and spherical indenter measurements, particularly for elastic modulus derived at small strains within the LVE range. However, the different loading conditions produced large differences in yield stress and other mechanical parameters at greater strain values within the nonlinear viscoelastic zone. Although indenter tests are more complicated to analyse and interpret, they have several advantages over a rheometer. A rheometer is limited to viscoelastic materials that flow, such as wet soils, but an indenter can be applied across a broad range of water contents including dry soils that fail by brittle fracture. Rheometers also require testing of pastes, whereas an indenter could be used on intact soil aggregates.

There is great scope to extend this research further. Deformation processes from an indenter on soils over a broad range of water contents need greater investigation to understand the loading and failure conditions. Differences in mechanical behaviour between soil pastes and intact specimens also needs to be explored. The dual approach could be applied to unravel processes involved in seedbed coalescence and aggregate stability, exploring impacts of texture, organic matter, hydrological stresses, and biology. Derived parameters will remove the elusiveness of soil hydromechanical processes that drive aggregate coalescence and breakdown, providing valuable information for process-based models of soil structure dynamics.

Declaration of competing interest

The authors have no conflict of interest involving this study and the findings reported in this paper.

Acknowledgements

Funding from the NJ faculty at the Swedish University of Agricultural Sciences (SLU) is acknowledged for partly funding RH's Ph.D. work. PH acknowledges funding from UKRI (BB/L026058/1, ES/T003073/1, NE/S009167/1) that supported background research that led to this study. This research was partly funded by the Faculty of Natural Resources and Agricultural Sciences (NJ Faculty) of the Swedish University of Agricultural Sciences.

Appendix A. Supporting information

Supplementary data associated with this article can be found in the online version at doi:10.1016/j.still.2022.105467.

References

Aguiar, C.B., Maghous, S., 2018. Micromechanical approach to effective viscoelastic properties of micro-fractured geomaterials. Int. J. Numer. Anal. Methods 42 (16), 2018–2046. https://doi.org/10.1002/nag.2847.

Amidon, G.E., Houghton, M.E., 1995. The effect of moisture on the mechanical and powder flow properties of microcrystalline cellulose. Pharm. Res. 12 (6), 923–929. https://doi.org/10.1023/A:1016233725612.

Baltá-Calleja, F.J., Cagiao, M.E., Adhikari, R., Michler, G.H., 2004. Relating microhardness to morphology in styrene/butadiene block copolymer/polystyrene blends. Polymer 45 (1), 247–254. https://doi.org/10.1016/j.polymer.2003.10.089.

Barré, P., Hallett, P.D., 2009. Rheological stabilization of wet soils by model root and fungal exudates depends on clay mineralogy. Eur. J. Soil Sci. 60, 525–538. https://doi.org/10.1111/j.1365-2389.2009.01151.x.

Berli, M., Eggers, C.G., Accorsi, M.L., Or, D., 2006. Theoretical analysis of fluid inclusions for in situ soil stress and deformation measurements. Soil Sci. Soc. Am. J. 70, 1441–1452. https://doi.org/10.2136/sssaj2005.0171.

Bresson, L.M., Moran, C.J., 1995. Structural change induced by wetting and drying in seedbeds of a hardsetting soil with contrasting aggregate size distribution. Eur. J. Soil Sci. 46, 205–214. https://doi.org/10.1111/j.1365-2389.1995.tb01828.x.

Bresson, L.M., Moran, C.J., 2004. Micromorphological study of slumping in a hardsetting seedbed under various wetting conditions. Geoderma 118 (3–4), 277–288. https://doi.org/10.1016/S0016-7061(03)00212-X.
Bro, A.D., Stewart, J.P., Pradel, D.E., 2013. "Estimating undrained strength of clays from direct shear testing at fast displacement rates". In: Meehan, C.L., Pradel, D., Pando, M.A., Labuz, J.F. (Eds.), Proc., Geocongress 2013: Stability and Performance of Slopes and Embankments III. ASCE, San Diego, pp. 106–119. https://doi.org/10.1061732/9780784412787.012.
Canovic, E.P., Qing, B., Mijailovic, A.S., Jagielska, A., Whitfield, M.J., Kelly, E., Turner, D., Sahin, M., Van Vliet, K.J., 2016. Characterizing multiscale mechanical properties of brain tissue using atomic force microscopy, impact indentation, and rheometry. J. Vis. Exp. 115, e54201 https://doi.org/10.3791/54201.
Carminati, A., Kaestner, A., Ippisch, O., Koliji, A., Lehmann, P., Hassanein, R., Flühler, H., 2007. Water flow between soil aggregates. Transp. Porous Media 68 (2), 219–236. https://doi.org/10.1007/s11242-006-9041-z.
Carminati, A., Kaestner, A., Lehmann, P., Fluhler, H., 2008. Unsaturated water flow across soil aggregate contacts. Adv. Water Resour. 31 (9), 1221–1232. https://doi.org/10.1016/j.advwatres.2008.01.008.
Chan, H.M., Lawn, B.R., 1988. Indentation deformation and fracture of sapphire. J. Am. Ceram. Soc. 71 (1), 29–35. https://doi.org/10.1111/j.1151-2916.1988.tb05756.x.
Chandrasekhar, P., Kreiselmeier, J., Schwen, A., Weninger, T., Julich, S., Feger, K.-H., Schwärzel, K., 2018. Why we should include soil structural dynamics of agricultural soils in hydrological models. Water 10 (12), 1862. https://doi.org/10.3390/w10121862.
Chang, C., Garrido, M.A., Ruiz-Hervias, J., Zhang, Z., Zhang, L. l, 2018. Representative stress-strain curve by spherical indentation on elastic-plastic materials. Adv. Mater. Sci. Eng. 2018, 8316384. https://doi.org/10.1155/2018/8316384.
Chen, D.T.N., Wen, Q., Janmey, P.A., Crocker, J.C., Yodh, A.G., 2010. Rheology of soft materials. Annu Rev. Condens. Matter Phys. 1 (1), 301–322. https://doi.org/10.1146/annurev-conmatphys-070909-104120.
Chen, S., Kong, L., Xu, G., 2018. An effective way to estimate the Poisson's ratio of silty clay in seasonal frozen regions. Cold Reg. Sci. Technol. 154, 74–84. https://doi.org/10.1016/j.coldregions.2018.06.003.
Chen, Z., Wang, X., Atkinson, A., Brandon, N., 2016. Spherical indentation of porous ceramics: Cracking and toughness. J. Eur. Ceram. Soc. 36 (14), 3473–3480. https://doi.org/10.1016/j.jeurceramsoc.2016.05.010.
Cheng, L., Xia, X., Scriven, L.E., Gerberich, W.W., 2005. Spherical-tip indentation of viscoelastic material. Mech. Mater. 37 (1), 213–226. https://doi.org/10.1016/j.mechmat.2004.03.002.
de Cagny, H., Fazilati, M., Habibi, M., Denn, M.M., Bonn, D., 2019. The yield normal stress. J. Rheol. 63 (2), 285–290. https://doi.org/10.1122/1.5063796.
Ettehadi, A., Tezcan, M., Altun, G., 2020. Rheological behavior of water-clay suspensions under large amplitude oscillatory shear. Rheol. Acta 59 (9), 665–683. https://doi.org/10.1007/s00397-020-01221-9.
Fatichi, S., Or, D., Walko, R., Vereecken, H., Young, M.H., Ghezzehei, T.A., Hengl, T., Kollet, S., Agam, N., Avissar, R., 2020. Soil structure is an important omission in earth system models. Nat. Commun. 11 (1), 522. https://doi.org/10.1038/s41467-020-14411-z.
Fecarotti, C., Celauro, C., & Pirrotta, A. (2012). Linear ViscoElastic (LVE) Behaviour of Pure Bitumen via Fractional Model. Siiv-5th International Congress - Sustainability of Road Infrastructures 2012, 53, 450–461. https://doi:10.1016/j.sbspro.2012.09.896.
Cseh, G., Chinh, N.Q., Juhász, A., 1998. Indentation curves and viscosity measurements on glasses. J. Mater. Sci. Lett. 17, 1207–1209. https://doi.org/10.1023/A:1006593727372.
Ghezzehei, T.A., Or, D., 2000. Dynamics of soil aggregate coalescence governed by capillary and rheological processes. Water Resour. Res. 36 (2), 367–379. https://doi.org/10.1029/1999wr900316.
Ghezzehei, T.A., Or, D., 2001. Rheological properties of wet soils and clays under steady and oscillatory stresses. Soil Sci. Soc. Am. J. 65 (3), 624–637. https://doi.org/10.2136/sssaj2001.653624x.
Hallett, P.D., Bird, N.R.A., Dexter, A.R., Seville, J.P.K., 1998. Investigation into the fractal scaling of the structure and strength of soil aggregates. Eur. J. Soil Sci. 49 (2), 203–211. https://doi.org/10.1046/j.1365-2389.1998. 00147.x.
Hallett, P.D., Newson, T.A., 2005. Describing soil crack formation using elastic-plastic fracture mechanics. Eur. J. Soil Sci. 56 (1), 31–38. https://doi.org/10.1111/j.1365-2389.2004.00652.x.
Holthusen, D., Batistão, A.C., Reichert, J.M., 2020. Amplitude sweep tests to comprehensively characterize soil micromechanics: brittle and elastic interparticle bonds and their interference with major soil aggregation factors organic matter and water content. Rheol. Acta 59 (8), 545–563. https://doi.org/10.1007/s00397-020-01219-3.
Holthusen, D., Pértile, P., Reichert, J.M., Horn, R., 2017. Controlled vertical stress in a modified amplitude sweep test (rheometry) for the determination of soil microstructure stability under transient stresses. Geoderma 295, 129–141. https://doi.org/10.1016/j.geoderma.2017.01.034.
Holthusen, D., Pértile, P., Reichert, J.M., Horn, R., 2019. Viscoelasticity and shear resistance at the microscale of naturally structured and homogenized subtropical soils under undefined and defined normal stress conditions. Soil Res. 191, 282–293. https://doi.org/10.1016/j.still.2019.04.014.
Khaidapova, D.D., Pestonova, E.A., 2007. Strength of interparticle bonds in soil pastes and aggregates. Eurasia Soil Sci. 40 (11), 1187–1192. https://doi.org/10.1134/S1064229307110063.
Khaidapova, D.D., Chestnova, V.V., Shein, E.V., Milanovskii, E.Y., 2016. Rheological properties of typical chernozems (Kursk Oblast) under Different Land Uses. Eurasia Soil Sci. 49, 890–897. https://doi.org/10.1134/S1064229316080044.
Keller, T., Ruiz, S., Stettler, M., Berli, M., 2016. Determining Soil Stress beneath a Tire: measurements and Simulations. Soil Sci. Soc. Am. J. 80 (3), 541–553. https://doi.org/10.2136/sssaj2015.07.0252.
Koch, T., Seidler, S., 2009. Correlations between indentation hardness and yield stress in thermoplastic polymers. Strain 45 (1), 26–33. https://doi.org/10.1111/j.1475-1305.2008.00468.x.
Lau, H.K., Rattan, S., Fu, H., Garcia, C.G., Barber, D.M., Kiick, K.L., Crosby, A.J., 2020. Micromechanical properties of microstructured elastomeric hydrogels. Macromol. Biosci. 20 (5), e1900360 https://doi.org/10.1002/mabi.201900360.
Lee, E.H., Radok, J.R.M., 1960. The contact problem for viscoelastic bodies. ASME. J. Appl. Mech. 438–444. https://doi.org/10.1115/1.3644020.
Likos, W.J., Lu, N., 2004. Hysteresis of capillary stress in unsaturated granular soil. J. Eng. Mech. ASCE 130 (6), 646–655. https://doi.org/10.1061/(ASCE)0733-9399(2004)130:6(646).
Logsdon, S., Berli, M., Horn, R., 2013. Quantifying and modeling soil structure dynamics. In: Logsdon, S., Berli, M., Horn, R. (Eds.), In Quantifying and Modeling Soil Structure Dynamics. https://doi.org/10.2134/advagricsystmodel3.c1.
Markgraf, W., Horn, R., Peth, S., 2006. An approach to rheometry in soil mechanics—Structural changes in bentonite, clayey and silty soils. Soil Til. Res. 91 (1–2), 1–14. https://doi.org/10.1016/j.still.2006.01.007.
Matsushi, Y., Matsukura, Y., 2006. Cohesion of unsaturated residual soils as a function of volumetric water content. B Eng. Geol. Environ. 65 (4), 449–455. https://doi.org/10.1007/s10064-005-0035-9.
Naveed, M., Brown, L.K., Raffan, A.C., George, T.S., Bengough, A.G., Roose, Sinclair, I., Koebernick, N., Cooper, L., Hallett, P.D., 2018. Rhizosphere-scale quantification of hydraulic and mechanical properties of soil impacted by root and seed exudates. Vadose Zone J. 17, 170083 https://doi.org/10.2136/vzj2017.04.0083.
Naveed, M., Brown, L.K., Raffan, A.C., George, T.S., Bengough, A.G., Roose, T., Sinclair, I., Koebernick, N., Cooper, L., Hackett, C.A., Hallett, P.D., 2017. Plant exudates may stabilize or weaken soil depending on species, origin and time. Eur. Soil Sci. 68, 806–816. https://doi.org/10.1111/ejss.12487.
Nimmo, J.R., Perkins, K.S., Plampin, M.R., Walvoord, M.A., Ebel, B.A., Mirus, B.B., 2021. Rapid-response unsaturated zone hydrology: small-scale data, small-scale theory, Big Problems. Front. Earth Sci. 9 https://doi.org/10.3389/feart.2021.613564.
Or, D., Berli, M., Eggers, C.G., Accorsi, M.L., 2006. Linking soil micro-mechanics and hydraulic conductivity. In: Horn, R., et al. (Eds.), Sustainability—Its Impact on Soil Management and Environment. Catena, Reiskirchen, Germany, pp. 59–70.
Or, D., Ghezzehei, T.A., 2002. Modeling post-tillage soil structural dynamics: a review. Soil Til. Res. 64 (1–2), 41–59. https://doi.org/10.1016/s0167-1987(01)00256-2.
Orbach, D.N., Rattan, S., Hogan, M., Crosby, A.J., Brennan, P.L.R., 2019. Biomechanical properties of female dolphin reproductive tissue. Acta Biomater. 86, 117–124. https://doi.org/10.1016/j.actbio.2019.01.012.
Pathak, S., Kalidindi, S.R., 2015. Spherical nanoindentation stress–strain curves. Adv. Mater. Res-Switz. 91, 1–36. https://doi.org/10.1016/j.mser.2015.02.001.
Persson, E., 2017. Empirical correlation between undrained shear strength and preconsolidation pressure in Swedish soft clays.
Pires, L.F., Cassaro, F.A.M., Reichardt, K., Bacchi, O.O.S., 2008. Soil porous system changes quantified by analyzing soil water retention curve modifications. Soil Til. Res. 100 (1–2), 72–77. https://doi.org/10.1016/j.still.2008.04.007.
Pértile, P., Holthusen, D., Gubiani, P.I., Reichert, J.M., 2018. Microstructural strength of four subtropical soils evaluated by rheometry: properties, difficulties and opportunities. Sci. Agric. 75, 154–162. https://doi.org/10.1590/1678-992x-2016-0267.
Polio, S.R., Kundu, A.N., Dougan, C.E., Birch, N.P., Aurian-Blajeni, D.E., Schiffman, J.D., Peyton, S.R., 2018. Cross-platform mechanical characterization of lung tissue. PLoS One 13 (10), e0204765. https://doi.org/10.1371/journal.pone.0204765.
Roger-Estrade, J., Richard, G., Dexter, A.R., Boizard, H., De Tourdonnet, S., Bertrand, M., Caneill, J., 2009. Integration of soil structure variations with time and space into models for crop management. A review. Agron. Sustain. Dev. 29, 135–142. https://doi.org/10.1051/agro:2008052.
Salager, S., Nuth, M., Ferrari, A., Laloui, L., 2013. Investigation into water retention behaviour of deformable soils. Can. Geotech. J. 50 (2), 200–208. https://doi.org/10.1139/cgj-2011-0409.
Stepniewska, M., Januchta, K., Zhou, C., Qiao, A., Smedskjaer, M.M., Yue, Y., 2020. Observation of indentation-induced shear bands in a metal−organic framework glass. Proc. Natl. Acad. Sci. USA 117 (19), 10149–10154. https://doi.org/10.1073/pnas.2000916117.
Stoppe, N., Horn, R., 2017. How far are rheological parameters from amplitude sweep tests predictable using common physicochemical soil properties. J. Phys. Conf. Ser. 790, 012032 https://doi.org/10.1088/1742-6596/790/1/012032.
Sun, B., Dennis, P.G., Newsham, K.K., Hopkins, D.W., Hallett, P.D., 2017. Gelifluction and thixotropy of maritime antarctic soils: small-scale measurements with a rotational rheometer. Permafr. Periglac. 28 (1), 314–321. https://doi.org/10.1002/ppp.1886.
Taylor, L.J., Papadopoulos, D.G., Dunn, P.J., Bentham, A.C., Mitchell, J.C., Snowden, M.J., 2004. Mechanical characterisation of powders using nanoindentation. Powder Technol. 143–144, 179–185. https://doi.org/10.1016/j.powtec.2004.04.012.
Transtrum, M.K., Qiu, P., 2016. Bridging mechanistic and phenomenological models of complex biological systems. PLoS Comput. Biol. 12 (5), e1004915 https://doi.org/10.1371/journal.pcbi.1004915.
Vachhani, S.J., Doherty, R.D., Kalidindi, S.R., 2013. Effect of the continuous stiffness measurement on the mechanical properties extracted using spherical nanoindentation. Acta Mater. 61 (10), 3744–3751. https://doi.org/10.1016/j.actamat.2013.03.005.

Vaidyanathan, R., Dao, M., Ravichandran, G., Suresh, S., 2001. Study of mechanical deformation in bulk metallic glass through instrumented indentation. Acta Mater. 49 (18), 3781–3789. https://doi.org/10.1016/S1359-6454(01)00263-4.

Vardanega, P.J., Bolton, M.D., 2013. Stiffness of CLays and Silts: Normalizing Shear Modulus and Shear Strain. J. Geotech. Geoenviron. 139 (9), 1575–1589. https://doi.org/10.1061/(Asce)Gt.1943-5606.0000887.

Vogel, H.J., Weller, U., Schlüter, S., 2010. Quantification of soil structure based on Minkowski functions. Comput. Geosci. 36 (10), 1236–1245. https://doi.org/10.1016/j.cageo.2010.03.007.

Yoshida, S., Hallett, P.D., 2008. Impact of hydraulic suction history on crack growth mechanics in soil. Water Resour. Res. 44, W00C01. https://doi.org/10.1029/2007WR006055.

Yun, T.S., Santamarina, J.C., Ruppel, C., 2007. Mechanical properties of sand, silt, and clay containing tetrahydrofuran hydrate. J. Geophys. Res. 112, B04106. https://doi.org/10.1029/2006JB004484.

Zafar, U., Hare, C., Hassanpour, A., Ghadiri, M., 2021. Effect of strain rate on powder flow behaviour using ball indentation method. Powder Technol. 380, 567–573. https://doi.org/10.1016/j.powtec.2020.11.057.